Supplement

Observational Uncertainties

Figure S1. One standard deviation uncertainty in OCO-2 SIF for January 2015. Dark red grid cells have no observations.
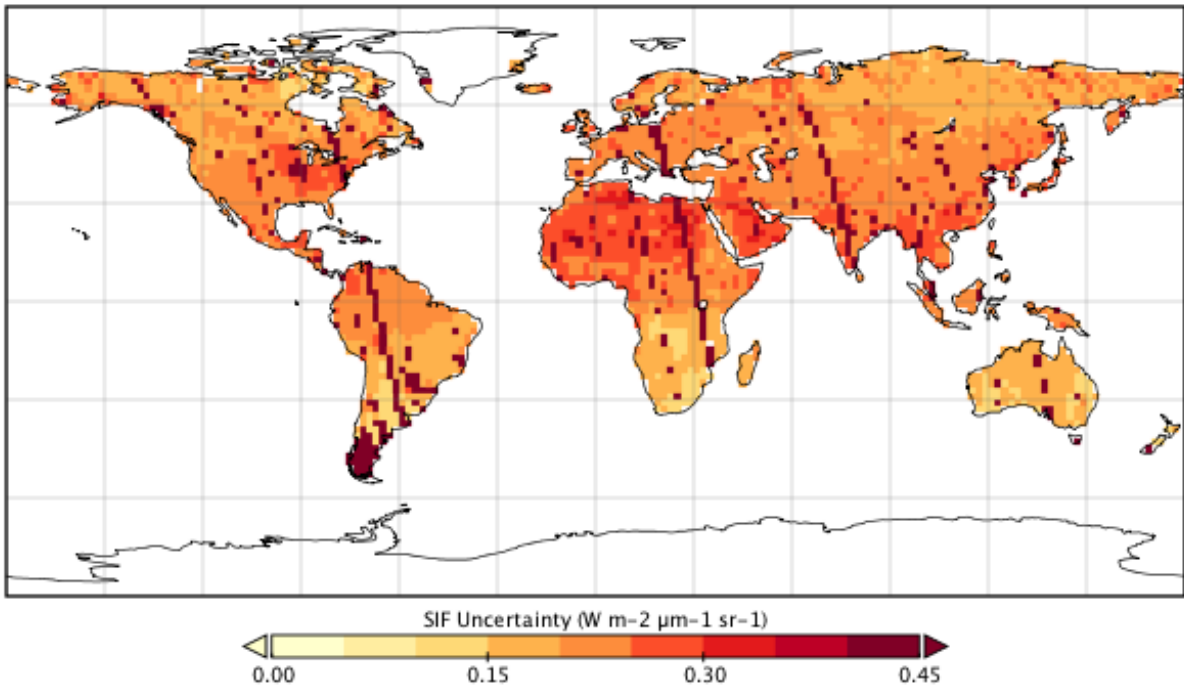
Figure S2. One standard deviation uncertainty in OCO-2 SIF for July 2015. Dark red grid cells have no observations.

Model-Observed Fit
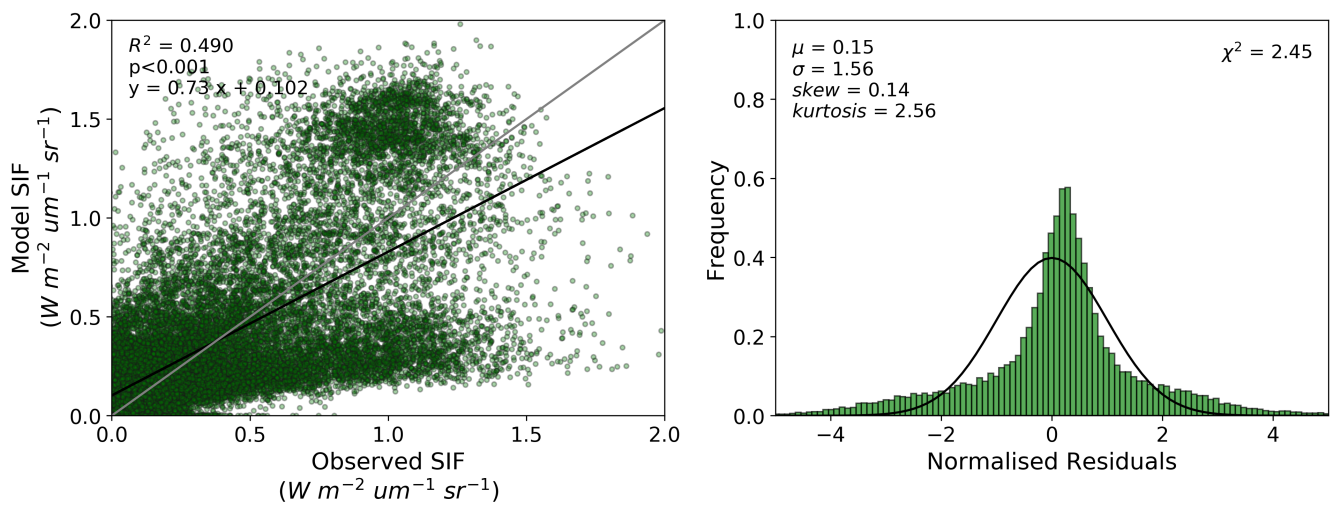
Figure S3. Prior model-observed fit and normalized residuals (modelled minus observed SIF divided by observational uncertainty) over the calibration period (SIF_{prior}).
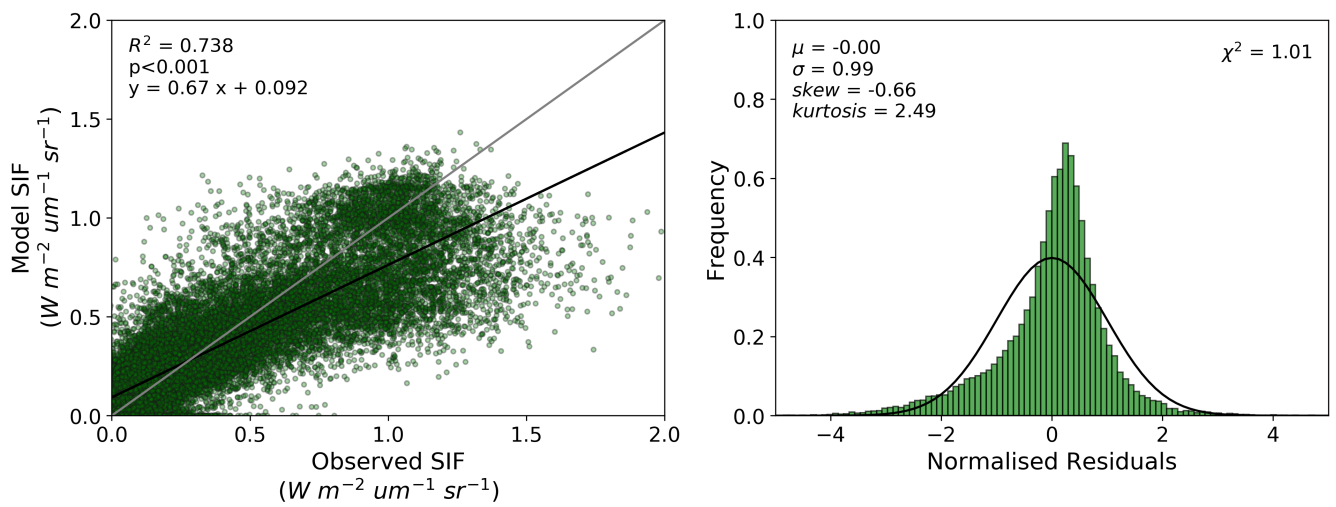
Figure S4. Posterior model-observed fit and normalized residuals (modelled minus observed SIF divided by observational uncertainty) over the calibration period (SIF_{post}).
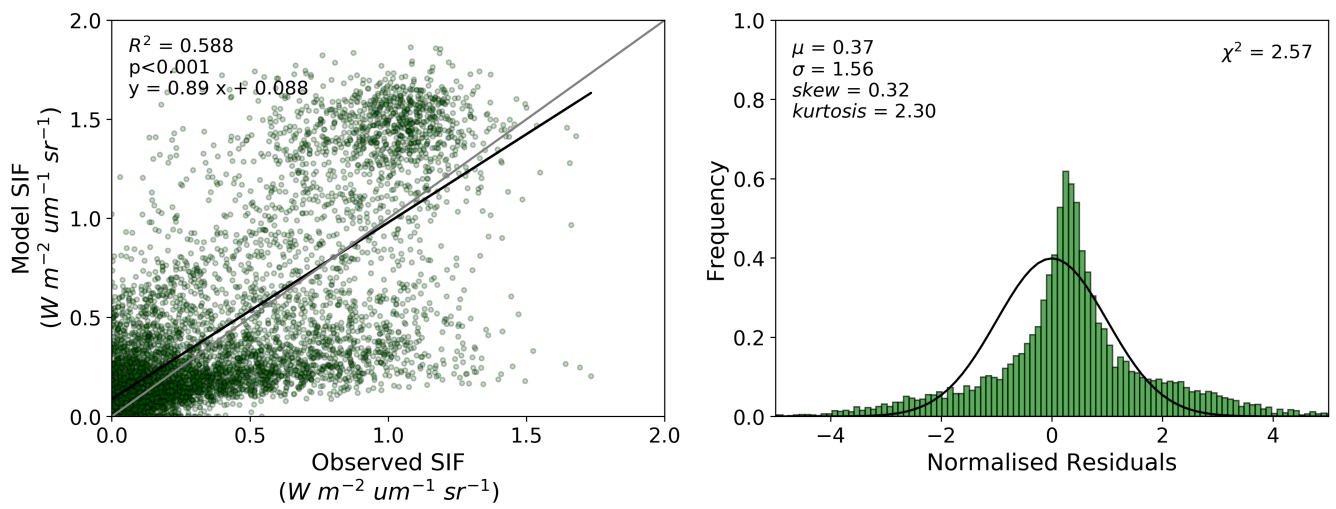
Figure S5. Prior model-observed fit and normalized residuals (modelled minus observed SIF divided by observational uncertainty) over the validation period.
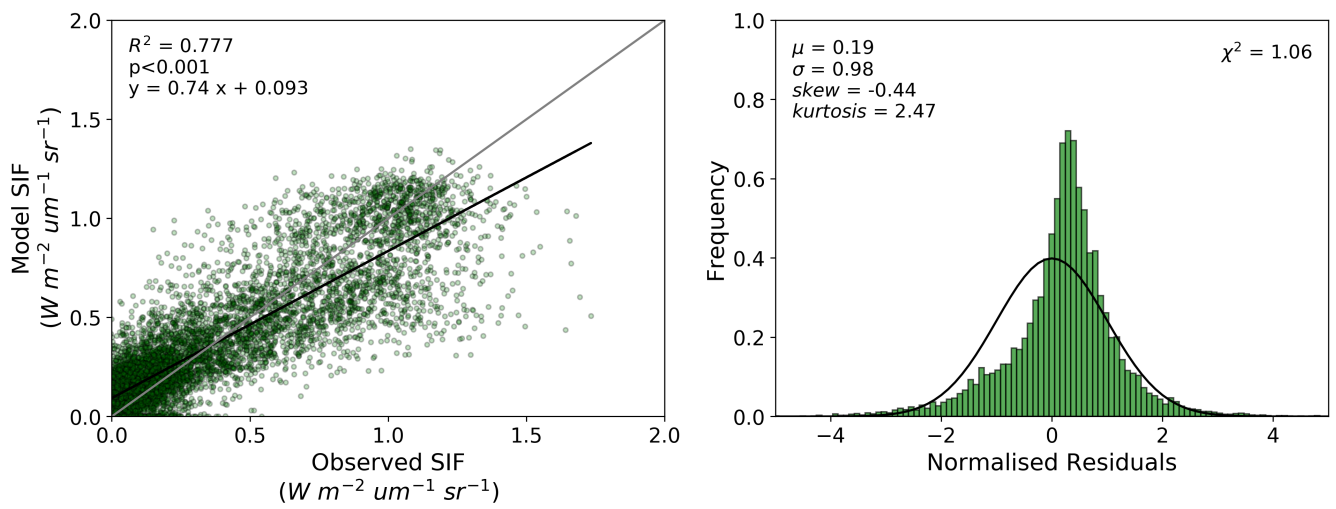
Figure S6. Posterior model-observed fit and normalized residuals (modelled minus observed SIF divided by observational uncertainty) over the validation period.

Model-Observed Mismatch
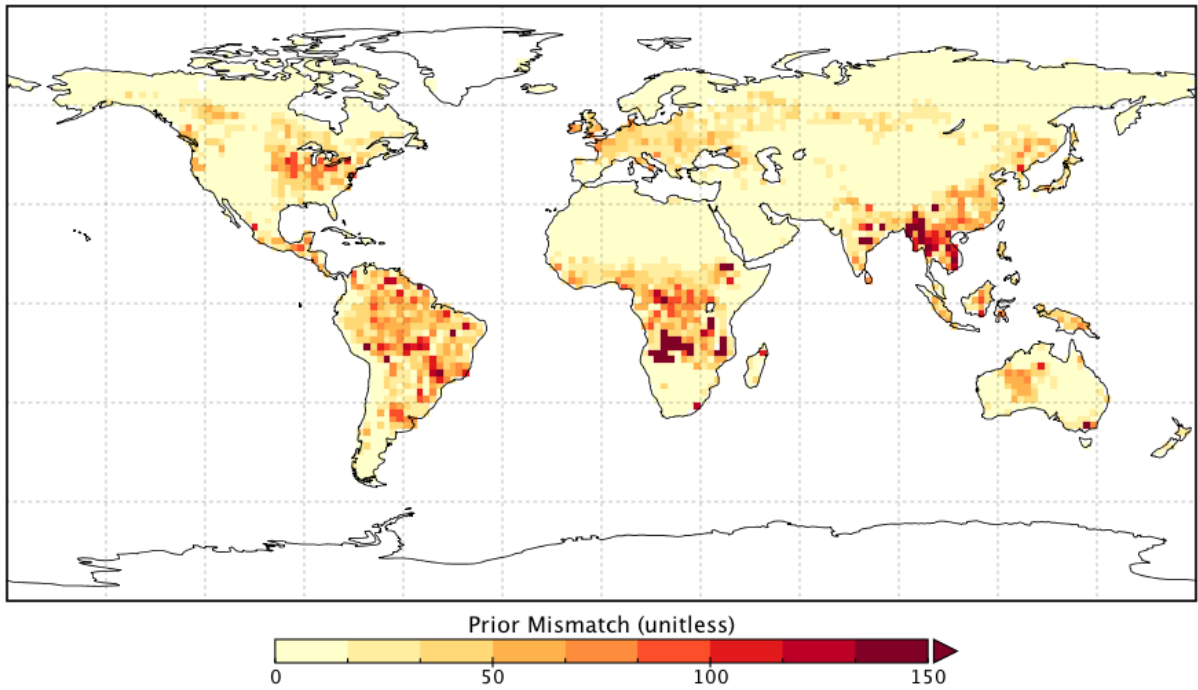
Figure S7. Annual total mismatch between the observed SIF and prior model SIF (SIF_{prior}).
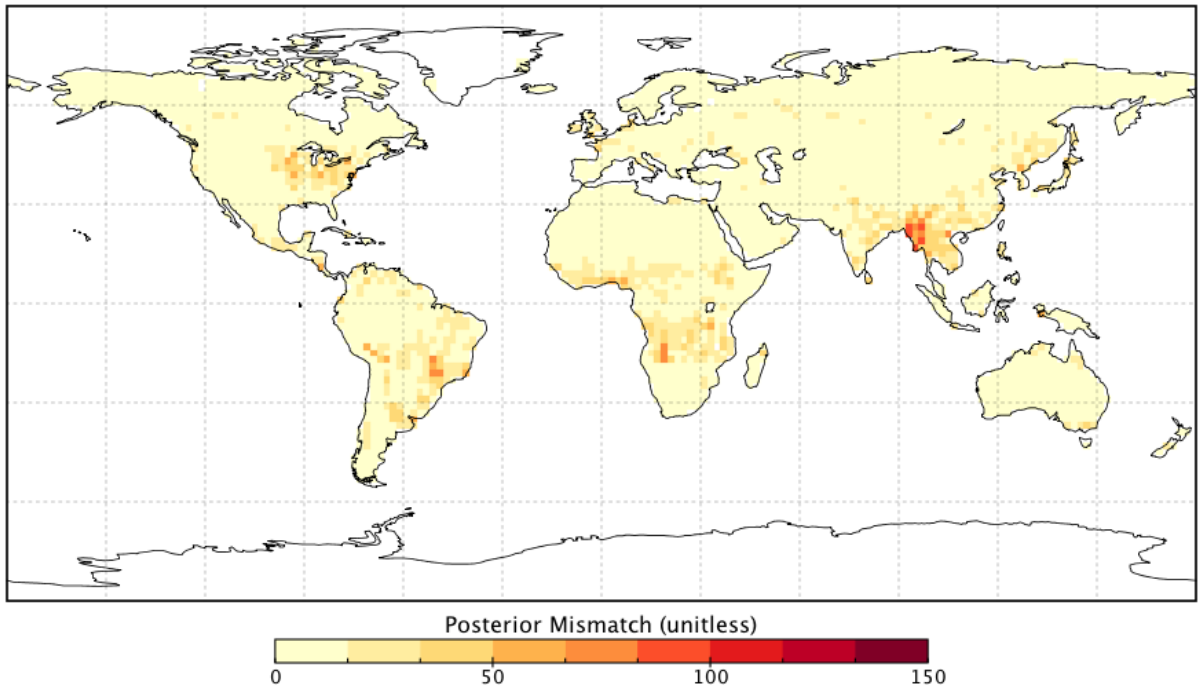
Figure S8. Annual total mismatch between the observed SIF and posterior model SIF (SIF_{post}).
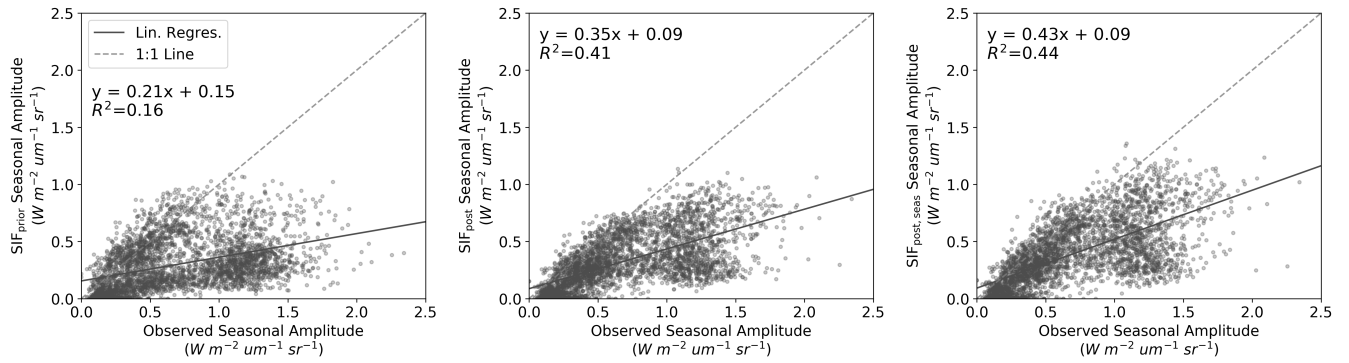
Figure S9. Model versus observed seasonal amplitude of SIF for the prior model (left), SIF-optimized model (middle), and SIF-optimized model with seasonally varying C_{ab} and V_{cmax} parameters (right). Shown on each plot is a 1:1 line (grey) and linear regression line (blue) with the associated equation. Also shown is the mean ratio between the model and observed seasonal amplitude.

Regional Model-Observed Differences
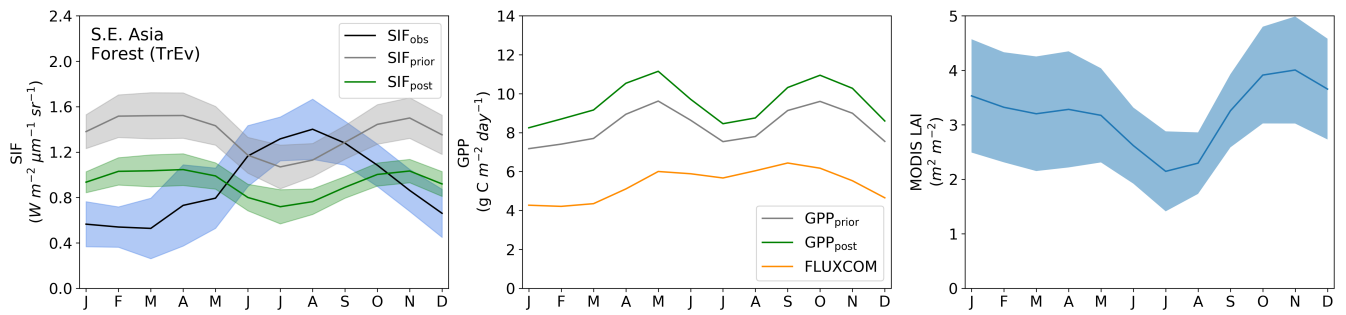
Figure S10. Regional patterns of SIF (left), GPP (center) and LAI (right) over mainland south-east Asia only for model grid cells with TrEv as the dominant PFT (see Fig. S11). The shading represents one sigma spread of data points in the selected region and month.
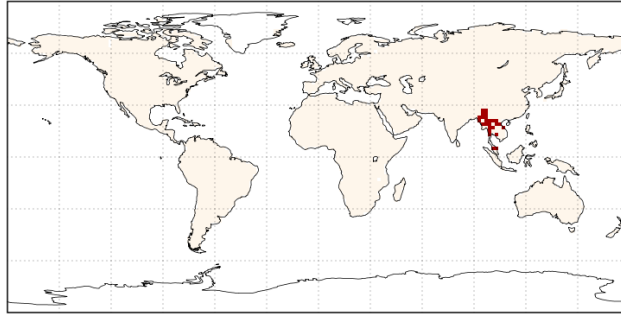
Figure S11. Model grid points selected for the regional analysis of mainland south-east Asia tropical forest.
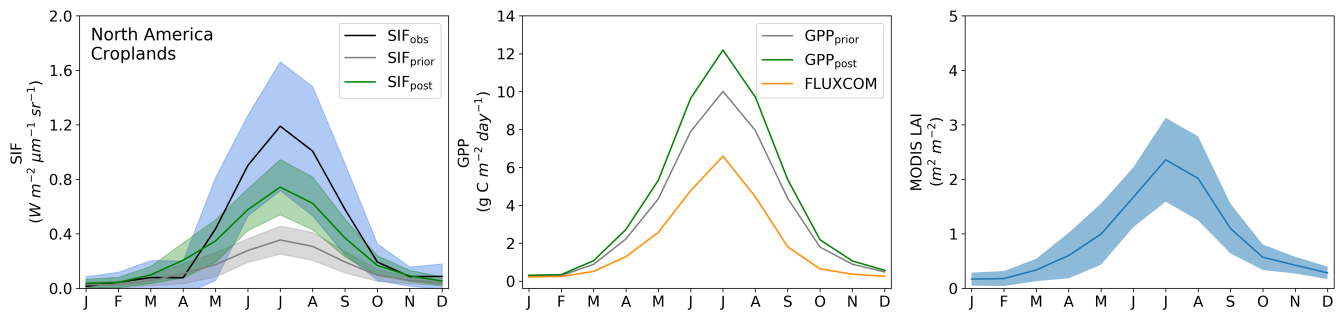
Figure S12. Regional patterns of SIF (left), GPP (center) and LAI (right) over North America croplands only for model grid cells with Crop as the dominant PFT (see Fig. S13). The shading represents one sigma spread of data points in the selected region and month.
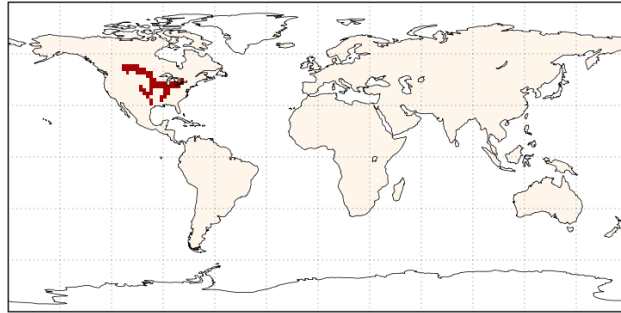
Figure S13. Model grid points selected for the regional analysis of North American croplands.
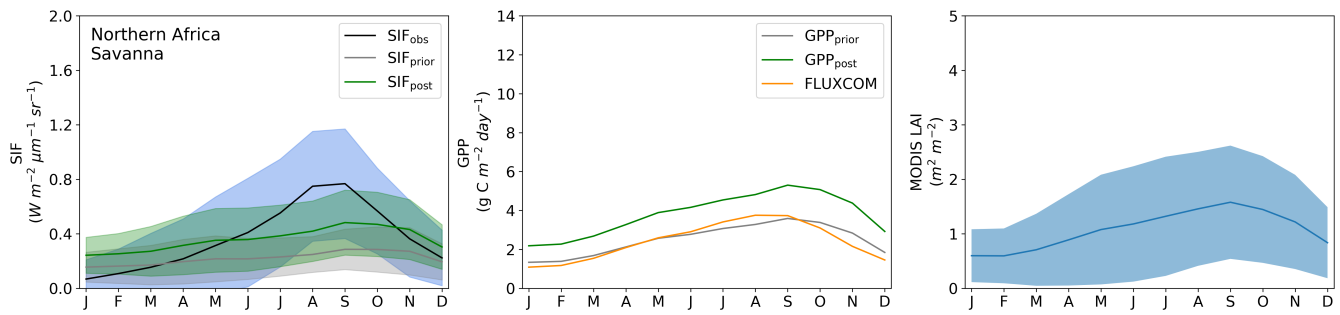
Figure S14. Regional patterns of SIF (left), GPP (center) and LAI (right) over north Africa savanna only for model grid cells with C4 grass as the dominant PFT (see Fig. S15). The shading represents one sigma spread of data points in the selected region and month.
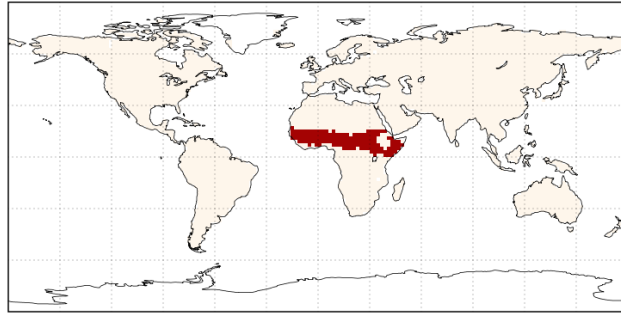
Figure S15. Model grid points selected for the regional analysis of north African savanna.

Spatiotemporal Patterns of GPP, SIF, V_{cmax} and C_{ab}
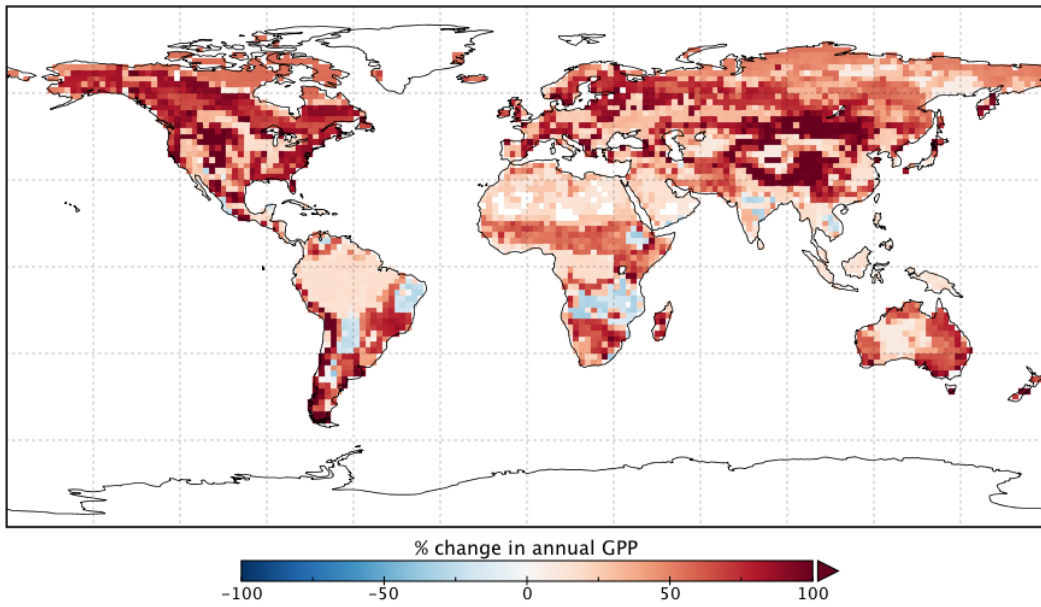
Figure S16. Percentage change in annual mean GPP rate for 2015 following optimization with SIF relative to GPP$_{prior}$.
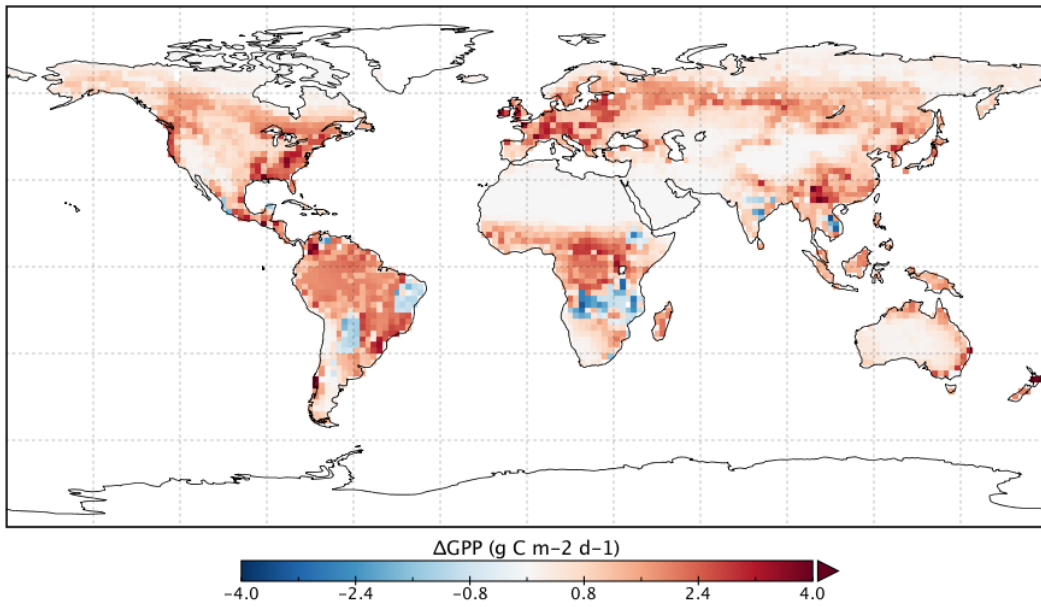
Figure S17. Change in annual mean GPP for 2015 following optimization with SIF relative to GPP_prior.
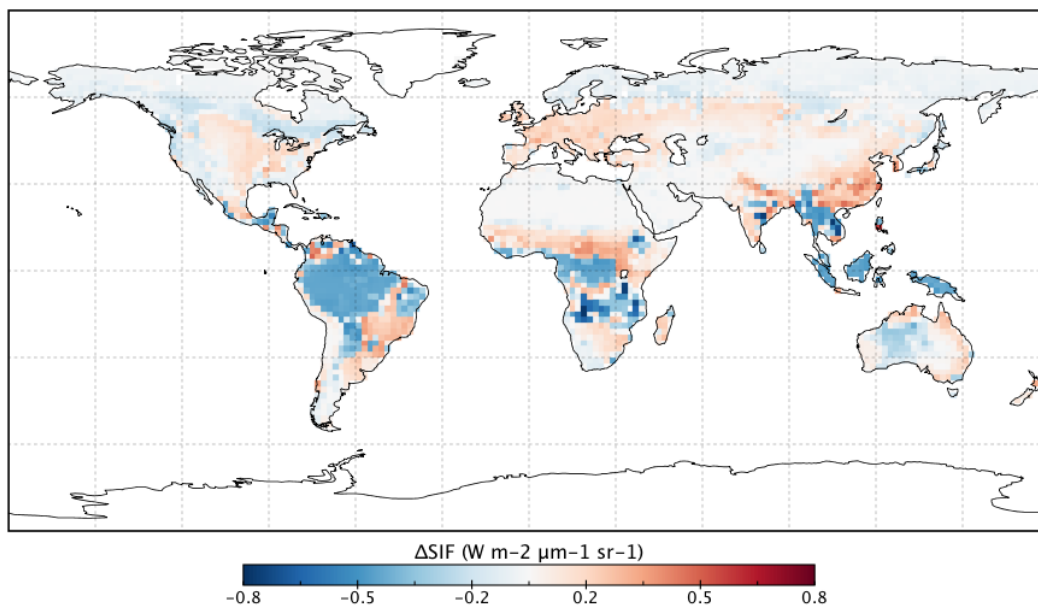
Figure S18. Change in annual mean SIF for 2015 following optimization with SIF relative to SIF$_{prior}$.
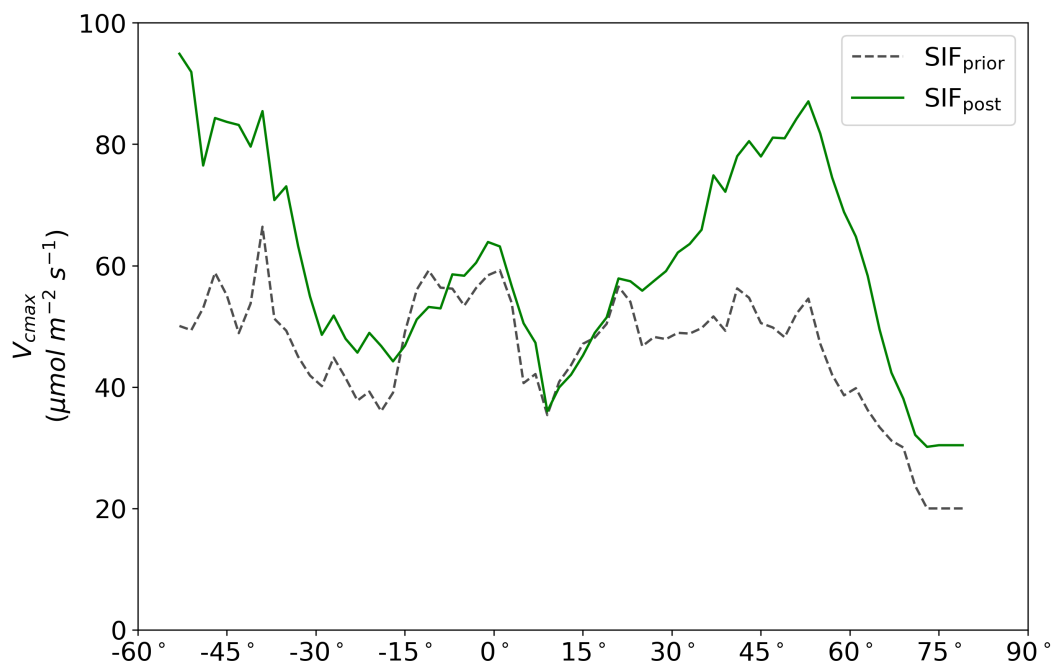
Figure S19. Latitudinal average of mapped maximum carboxylation capacity at 25°C, V_{cmax}, parameter values for the prior and posterior cases.
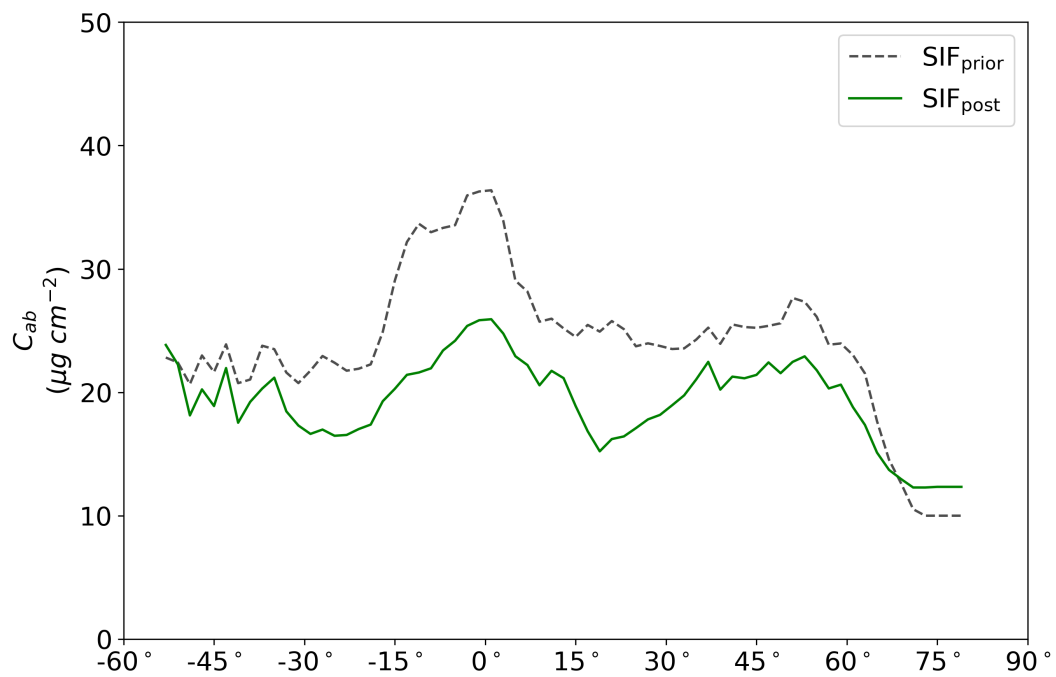
Figure S20. Latitudinal average of mapped chlorophyll content, C_{ab}, parameter values for the prior and posterior cases.